International Journal of
Thermodynamics and Chemical Kinetics

ISSN: 2456-6977
Volume 10, Issue 1, 2024
January–June
DOI (Journal): 10.37628/IJTCK

https://journalspub.com/journal/IJTCK/

Review IJTCK

Modeling the Biokinetic of Crude Oil Degradation in Loamy Soil Using the Citrus Sinensis of Flavedo Part

Ukpaka, Chukwuemeka Peter[1,*], Vidose-Eli, Edomeme Amenawon[2]

Abstract

The biokinetic parameters of crude oil degradation using Citrus sinensis of flavedo part was investigated in loamy soil environment. Mathematical models were developed for the purpose of determining the biokinetic parameters of the k_1 (Total Petroleum Hydrocarbon), maximum specific rate of TPH remediation and dissociation constant of the TPH remediation on the effect of remediant dosage on the polluted loamy soil environment. The effect of the remediants were monitored for sun-dried and room-dried samples of the citrus sinensis of the flavedo part. The application of Michaelis Menten, Lineweaver–Burk plot and first order reaction kinetic was used in the determination of the biokinetic parameters as demonstrated in this research. However, decrease in TPH was experienced with increase in time and the k_s ranges from – 39285.714 $(ppm)^{-1}$ to 18434 $(ppm)^{-1}$ whereas the R_{max} value ranges from –1250 $(ppm/day)^{-1}$ to 2083.33 $(ppm/day)^{-1}$. In $S_{TPH(t)}$ ranges from 10.271 to 10.931 and k1 value ranges from – 0.0561 to – 0.0382 for room-dried samples whereas for sun-dried k_1 value ranges from –0.0531 to 0.0068 and in $S_{TPH(t)}$ value ranges from 10.269 to 10.865. These biokinetic parameters are influenced by the effect of dosage and effectiveness of the microbes to remedy the polluted loamy soil environment.

Keywords: Biokinetic, modeling, crude oil, degradation, loamy soil citrus sinensis

INTRODUCTION

The application of bioremediant for the treatment of contaminated soil environment is not new, however, continuous research to identify other components or materials that are capable of degrading the contaminant and generating components that are environmentally friendly is of utmost importance.

Crude oil spill and inadequate treatment of the effluent water generated by the oil companies, indeed influence the ecosystem and there is need to remedy the contaminated soil environment for restoration of the soil integrity [1–3]. Research conducted by various research groups revealed that application of chemical remediant may remove the pollution at the initial stage but would have adverse effect reacting and generating worse chemicals or toxins into the soil environment [4, 5]. For this reason, current researchers have condemned the concept of chemical treatment for soil remediation [6]. Physical methods of remediation, though favorable because no likely environmental hazard is generated, takes extremely long time to achieve a reasonable degree of remediation and as such has not been so widely used [7]. Currently, biological treatment of the soil is widely advocated since all the substances produced are environmentally friendly and the process is cost effective [5–10].

***Author for Correspondence**
Ukpaka, Chukwuemeka. Peter
E-mail: peter.ukpaka@ust.edu.ng.

[1]Professor, Department of Chemical/Petrochemical Engineering, Rivers State University Port Harcourt
[2]Student, Department of Chemical/Petrochemical Engineering, Rivers State University Port Harcourt, Rivers State, Nigeria

Received Date: July 24, 2024
Accepted Date: July 31, 2024
Published Date: August 15, 2024

Citation: Ukpaka, Chukwuemeka Peter, Vidose-Eli, Edomeme Amenawon. Modeling the Biokinetic of Crude Oil Degradation in Loamy Soil Using the Citrus Sinensis of Flavedo Part. International Journal of Thermodynamics and Chemical Kinetics. 2024; 10(1): 25–50p.

On this note, there is need for continuous research on agro-based materials that can be suitable for bioremediation. Especially considering components classified as waste and converting them to items of value. This is the reason and focus of this research. Considering the high nutritional content of the orange fruit itself, it is optimistic that the peel (flavedo) would have a high potential to function effectively as a soil remediant [11–15].

The worldwide issues posed by environmental contamination, which are further intensified by petroleum operations, are of considerable magnitude, especially within the framework of climate change [16]. This phenomenon has resulted in a range of problems, including the buildup of harmful compounds in living organisms, contamination of aquatic ecosystems, degradation of soil composition and consistency, potential health concerns, disruptions in ecological equilibrium, and increased toxicity for both human beings and the environment. Despite the collective efforts of governmental bodies, companies, researchers, and many stakeholders, these issues continue to exist in several geographical areas. Hence, it is essential to ascertain sustainable remediation procedures, novel insights into remediation methodologies, and effective clean-up approaches to address these difficulties [17–20].

The efficacy of bio-remediation methods for oil spills relies on the capacity to develop and sustain favorable circumstances that promote increased rates of oil biodegradation in the affected ecosystem. Several scientific review publications have extensively examined a range of parameters that impact the rate of oil biodegradation. An essential prerequisite is the existence of bacteria with the requisite metabolic capacities [21–24]. To sustain optimum rates of development and hydrocarbon biodegradation in the presence of these microorganisms, it is essential to maintain appropriate levels of nutrients and oxygen, while also preserving a pH within the range of 6 to 9 [25]. Bioremediation success is significantly influenced by the physical and chemical properties of the oil, as well as the surface area covered by the oil. There exist two primary methodologies for oil spill bioremediation: (a) bioaugmentation, which involves the introduction of known oil-degrading bacteria to enhance the existing microbial community, and (b) biostimulation, which entails the stimulation of indigenous oil degraders by introducing nutrients or other growth-limiting co-substrates [26–30].

Materials and Methods

The orange fruit may be divided into two separate sections, as shown in Figure 1 the pericarp, sometimes referred to as the peel, skin, or rind, and the endocarp, which encompasses the pulp and juice sacs. The pericarp is composed of two distinct layers, namely the mesocarp, which is notable for its white color, thick consistency, and spongy feel, and the epicarp. The endocarp encompasses the pulp, which is organized into discrete pieces called juice sacs, often containing seeds. The seeds, which are often characterized by their light white color, flattened structure, and angular form, are frequently disposed of as refuse (Figure 1).

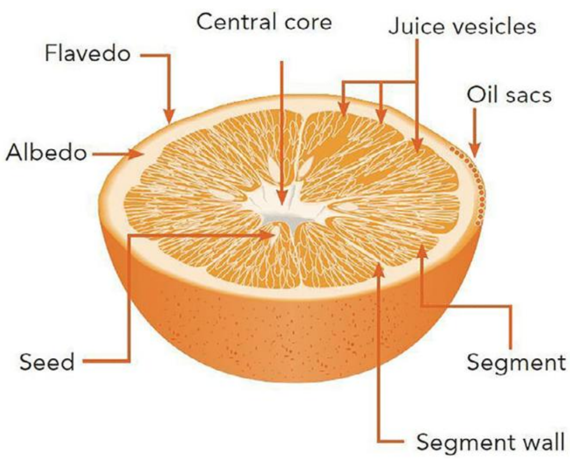

Figure 1. Structure of the Orange Fruit [2].

Kinetic Models

The Model: Material Balance

The model was based on the interaction between the microbes and the substrate (TPH) in bioreactor with the aid of the bio-stimulant (nutrient) added in it. The material balance equation is given as:

$$\begin{bmatrix} Rate\ of\ Mass \\ of\ TPH \\ into\ the \\ bioreactor \end{bmatrix} = \begin{bmatrix} The\ rate\ of\ mass \\ of\ the\ TPH \\ from\ the\ b \\ ioreactor \end{bmatrix} + \begin{bmatrix} The\ rate\ of\ mass\ of \\ TPH\ disappearing \\ due\ to\ chemical \\ reaction\ from\ the \\ bioreactor \end{bmatrix} + \begin{bmatrix} The\ rate\ of \\ mass\ of\ TPH \\ accummulated \\ within\ the\ control \\ volume \end{bmatrix} \quad (1)$$

The bioreactor set-up is a batch process, therefore, the rate of mass of TPH into the reactor is equal to the rate of mass of TPH from the reactor and both are equal to zero, i.e.

$$\begin{bmatrix} Rate\ of\ mass \\ of\ TPH\ into \\ the\ bioreactor \end{bmatrix} = \begin{bmatrix} Rate\ of\ Mass \\ of\ TPH\ from \\ the\ reactor \end{bmatrix} = 0 \quad (2)$$

Therefore, the equation (3.44) becomes

$$\begin{bmatrix} The\ rate\ of\ mass \\ of\ TPH\ accumulated \\ within\ the\ control \\ volume \end{bmatrix} = \begin{bmatrix} The\ rate\ of\ TPH \\ disappearance\ due \\ to\ biochemical\ reaction \\ from\ the\ reactor \end{bmatrix} \quad (3)$$

First Order Reaction

Considering the reaction medium of the crude oil, microorganism and loamy soil environment, we can assume the reaction mechanism of

$$[L] + [E] + [S] \rightarrow [P] + [E] + [L] \quad (4)$$

where, $[L]$ represents loamy soil sample, $[E]$ represents microorganism$[S]$ represents TPH.

The reactor demonstration of the process is shown in Figure 2.

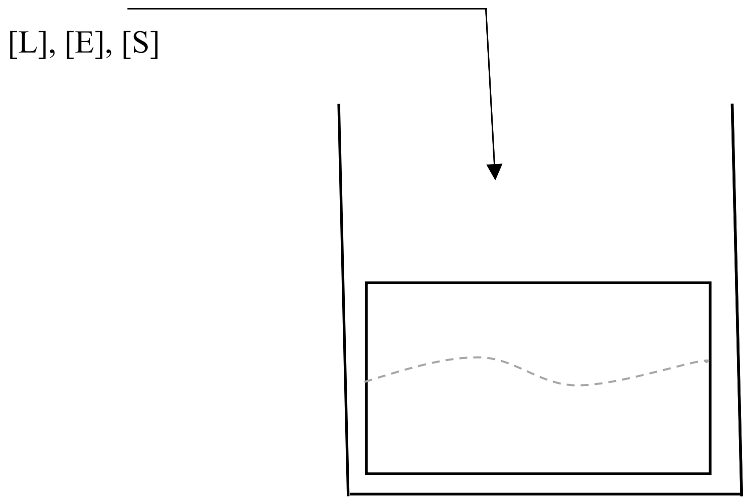

Figure 2. Simple bioreactor demonstrating reaction mechanism of the experimental setup.

Defining the mathematical expression of the Equation (1) we have

The rate of mass of the TPH into the bioreactor = $\varphi S_{TPH(0)}$ (5)

The rate of mass of the TPH from the bioreactor = φS_{TPH} (6)

The rate of mass of TPH disappearance due to biochemical reaction from the bioreactor $= -R_{TPH}V$ (7)

The rate of mass of TPH accumulation within the control volume = $\frac{d(S_{TPH}V)}{dt}$ (8)

Indeed, substituting equation (5), (6), (7), and (8) into Equation (1), we have

$$\varphi S_{TPH(0)} = \varphi S_{TPH} + (-R_{TPH}V) + \frac{d(S_{TPH}V)}{dt} \quad (9)$$

Since $\varphi S_{TPH(0)} = \varphi S_{TPH} = 0$ (10)

Therefore, Equation (10) becomes

$$\frac{d(S_{TPH}V)}{dt} = (-R_{TPH}V) \quad (11)$$

Equation (11) can be written as

$$= (-R_{TPH}V) = \frac{VdS_{TPH}}{dt} \quad (12)$$

Equation (12) shows that the volume of the reactor remains constant and the dividing through the Equation (12) by V, we have

$$-R_{TPH} = \frac{dS_{TPH}}{dt} \quad (13)$$

Considering that the concentration of the substrate is time dependent, the kinetic expression becomes

$$\frac{-dS_{TPH}}{dt} = k_1 S_{TPH}$$
$$\frac{-dC_{TPH}}{dt} = k_1 C_{TPH} \quad (14)$$

Indeed, the expression of equation (14) can be written as

$$-R_{TPH} = \frac{dS_{TPH}}{dt} = -k_1 S_{TPH}$$

Or

$$-R_{TPH} = \frac{dC_{TPH}}{dt} = -k_1 C_{TPH} \quad (15)$$

where, k_1 represents the TPH mitigation in the system, φ_0 represents the TPH initial concentration inlet volumetric rate of flow (kg/day), φ represents the TPH final concentration outlet volumetric rate of flow (kg/day), $S_{TPH(0)}$ represents the concentration initial of TPH (mg/kg), S_{TPH} represents the concentration final of TPH (mg/kg), V represents the bioreactor volume (m^3) and t represents the mitigation time (day).

From Equation (16) we have

$$\int_{S_{TPH(0)}}^{S_{TPH}} \frac{dS_{TPH}}{S_{TPH}} = -k_1 \int_0^t dt \tag{16}$$

$$\ln S_{TPH}{}_{S_{TPH(0)}}^{S_{TPH}} = -k_1 t_0^t \tag{17}$$

$$\ln S_{TPH} - \ln S_{TPH(0)} = -k_1(t-0) \tag{18}$$

$$\ln \frac{S_{TPH}}{S_{TPH(0)}} = -k_1 t \tag{19}$$

Equation (19) can be expressed as

$$S_{TPH(t)} = S_{TPH(0)} e^{-k_1 t} \tag{20}$$

Or

$$S_{TPH(t)} = S_{TPH(0)} exp(-k_1 t) \tag{21}$$

Equation (21) can be related to the straight-line curve relationship, thus,

$$y = mx + c$$

where, y = $S_{TPH(t)}$ represents the output, m =–k_1 represents the slope, c = $S_{TPH(0)}$represents the constant or intercept, t = x represents the coordinate $\ln S_{TPH(t)}$ against t can be established and the slope value m = k_1 and the intercept value of C= $S_{TPH(0)}$.

Kinetics of Michaelis Menten

The kinetics of the Michaelis Menten is derived from the application and concepts of Henry Model which examines the interaction of the substrate (TPH) degradation with the action of the microbes (enzymes) leading to the formation of enzyme-substrate complex. If the process is not inhibited by the possible factors as listed in the physiochemical parameters and other environment, there is tendency of the enzyme-substrate complex disintegrating to produce products and free enzyme. The above statement is illustrated in the Equation (22) as:

$$[E] + [S] \qquad [ES] \overset{k_3}{\rightarrow} [P] + [E_0] \tag{22}$$

where, E represents enzyme, S represents substrate (TPH), ES represents enzyme-substrate complex and E_0 represents free enzyme. The kinetics of Michelis Menten Model in general reveals that the specific rate of TPH degradation is given at

$$R = (R\_max\ [S])/(k\_s + [S]\ ) \ = \ (R\_max\ [C\_TPH\ ])/(k\_s + [C\_TPH\ ]\ ) \tag{23}$$

where, R represents the specific rate of substrate (TPH) concentration degradation, C_{TPH}, S represents the substrate (TPH) concentration, K_s represents the equilibrium constant of TPH R_{max} represents the maximum specific rate of TPH (substrate) concentration degradation.

Kinetics of the Lineweaver–Burk Plot

The kinetics of the Lineweaver–Burk plot is drawn from the concept of the Michael Menten's mathematical expression. This concept is found necessary because it is useful to relate the obtained model into the linear curve, which is important in establishing the slope value and the intercept value. This phenomenon will enhance the determination of functional parameters and coefficients as the case may be. Therefore, recalling Equation (23) and simplifying, we have

$$R = \frac{R_{max}[S]}{K_s + [S]}$$

$$\frac{1}{R_{TPH}} = \frac{k_{TPH}}{[R_{TPH}]_{max}[C_{TPH}]} + \frac{1}{[R_{TPH}]_{max}} \quad (24)$$

RESULTS AND DISCUSSION

The results obtained from the research are presented in Figures. Most of the results in Tables including some of the Laboratory data, are positioned in the appendices.

Effect of Time on TPH Concentration with Different Concentrate of Bio-stimulant

The effect of time and dosage concentration in mass of bio-stimulant was monitored on its performance on TPH mitigation as demonstrated in Figures 2 and 3 for the remediant of room and sun dried, respectively, of orange peel (Figure 3).

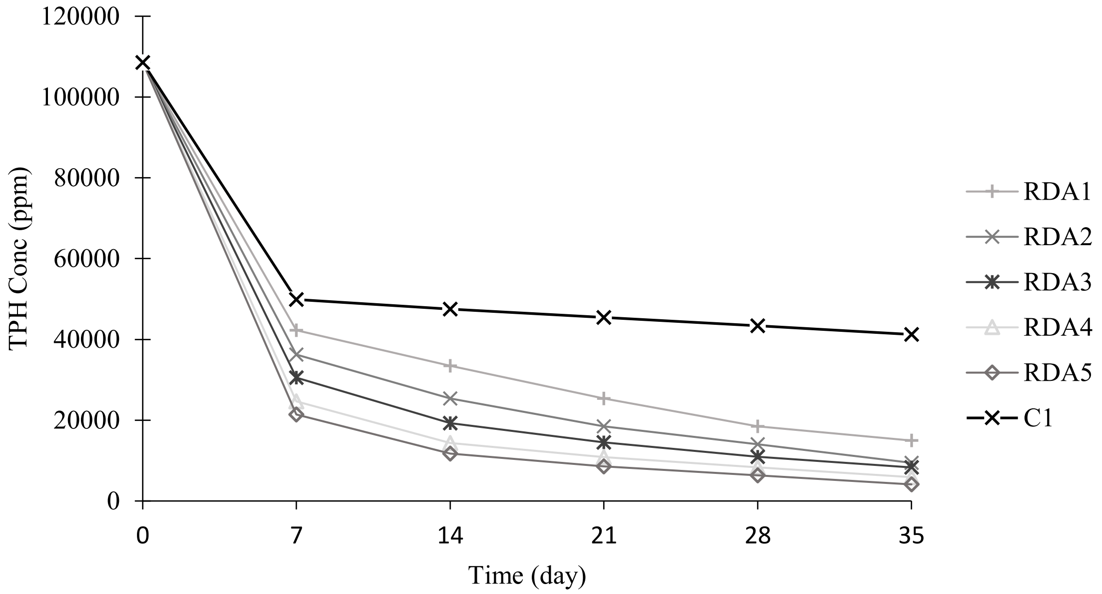

Figure 3. Plot of Remediation of TPH Concentration Versus Time.

Figure 3 shows the trend of the Total Petroleum Hydrocarbon (TPH) degradation based on the effect of time and action of the bio-stimulant of the room-dried peel of orange (*Citrus sinensis*). Figure 2 revealed a decrease in TPH concentration as the mass of the remediant (bio-stimulant) dosage. The effectiveness of the bio-stimulant yielded the recommendation on the order of mitigation as RDA5 > RDA4 > RDA3 > RDA2 > RDA1 > C1. Also, Figure 3 shows a decrease in the TPH concentration with increase in time.

Lineweaver–Burk Plot Determination of Functional Parameters for Room-Dried and Control Application

The figures presented in this area covers the parameters obtained because of room-dried application of orange peel. The Lineweaver–Burk plot was applied for the determination of the maximum specific rate of TPH degradation R_{max} and equilibrium constant of TPH degradation K_S and the result obtained are demonstrated from Figures 3 to Figure 8 for various dosage of 20 g, 40 g, 60 g, 80 g, and 100 g.

Figure 4 shows the Lineweaver–Burk plot of the reciprocal specific rate ($1/R_{TPH}$) of TPH mitigation with variation in substrate [S] from room-dried bio-stimulant (*Citrus sinensis*) peel of 20 g dosage. The maximum specific rate Rmax of TPH degradation and equilibrium constant K_S were determined since the Lineweaver–Burk plot theorem was obeyed. Recalling, the Lineweaver–Burk plot concept from Equation (25) thus:

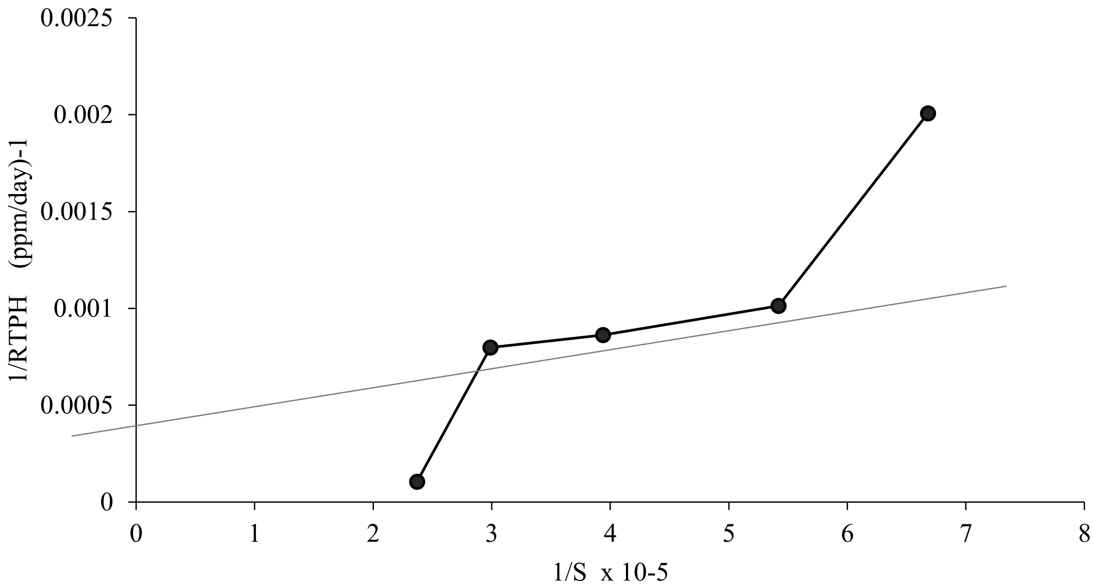

Figure 4. Lineweaver–Burk plot of $1/R_{TPH}$ vs. 1/[S] for bio-stimulant of room-dried of 20 g dosage.

$$\frac{1}{R} = \frac{k_s}{R_{max}[S]} + \frac{1}{R_{max}}$$

where $\frac{1}{R_{max}}$ = intercept and $\frac{k_s}{R_{max}}$ = slope

Therefore, reading off the graph, the intercept is 0.00048 $(ppm/day)^{-1}$ and the slope is calculated to be 8.85.

That is, $\frac{1}{R_{max}}$ = 0.00048 and R_{max} = 1/0.00048 = 2083.33 $(ppm/day)^{-1}$

since $\frac{k_s}{R_{max}} = slope$; It implies that $K_s = R_{max}$ (slope)

Reading off the graph, we calculate that slope = (0.001014 -- 0.000799)/(5.42 – 2.99) = 8.85

Therefore, K_s = 2083 * (8.85) = 18434 $(ppm)^{-1}$

Substituting values into the Lineweaver--Burk plot equation we have

$$\frac{1}{R} = \frac{18434}{2083.33[S]} + 4.8E + 04$$

And the Michaelis Menten equation for the 20 g dosage for the room-dried remediant is expressed as:

$R_{A1} = \frac{[R_{A1}]max[S]}{k_s+[S]}$, The equation obtained: $R_{A1} = \frac{2083.33*[S]}{18434+[S]}$

Using the Lineweaver–Burk plot in determining the TPH degradation functional parameters and coefficient with respect to substrate concentration, Figure 5 shows the plot of the reciprocal of specific rate ($1/R_{TPH}$) of TPH mitigation with variation in substrate [S] for a 40 g dosage of room-dried *Citrus sinensis* (orange) peel (bio-stimulant). Having obtained a negative intercept of the graph which is read off as the maximum specific rate R_{max} of TPH degradation, it signifies a non-compliance to the Lineweaver-Burk plot theorem. However, the concept of Ukpaka was adopted for the purpose of evaluating for the determination of the functional parameters and coefficient.

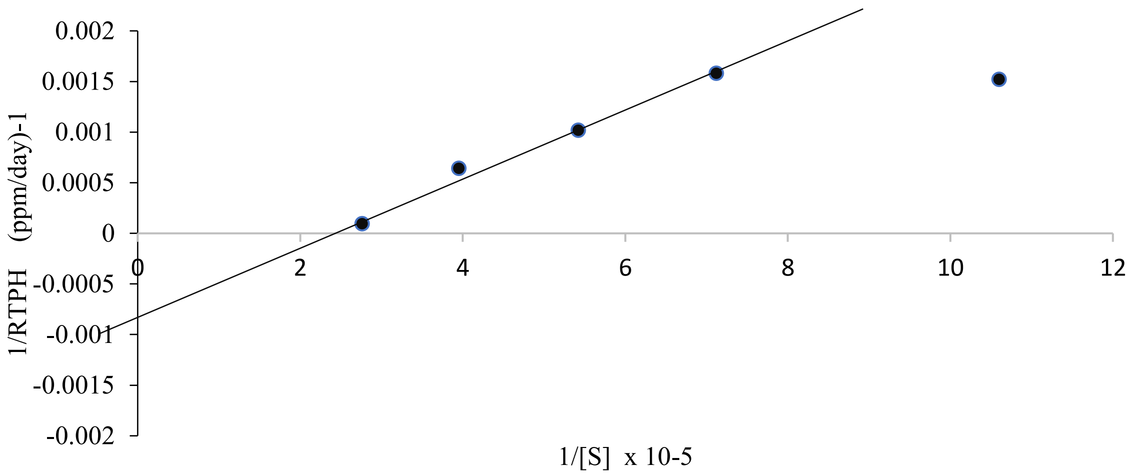

Figure 5. Lineweaver–Burk plot of $1/R_{TPH}$ vs. 1/[S] for bio-stimulant of room-dried of 40 g dosage.

Recalling, the Lineweaver–Burk plot concept from Equation (25) thus:

$$\frac{1}{R} = \frac{k_s}{R_{max}[S]} + \frac{1}{R_{max}}$$

where $\frac{1}{R_{max}}$ = intercept and $\frac{k_s}{R_{max}}$ = slope.

From Figure 4, we read off the intercept as –0.00084.

Therefore, $\frac{1}{R_{max}}$ = –0.00084 and, R_{max} = –1/0.00084 = –1190.47619

Since $\frac{k_s}{R_{max}} = slope$ then $K_s = R_{max}$ * (slope)

But the slope is computed as: slope = (0.00158 -- 0.00102)/(7.12 -- 5.42) x 10^{-5} = 33.

Substituting values of R_{max} and slope into the equation, we have:

Ks = –1190.47619 * (33) = –39285.7143 $(ppm)^{-1}$

Substituting values into the Michealis Menten equation as expressed as stated,

$$R_{A2} = \frac{[R_{A2}]_{max}[S]}{k_s + [S]}$$

For the 40 g dosage of remediant room dried we have

$$R_{A2} = \frac{-1190.48 * [S]}{-39285.71 + [S]}$$

Similarly, for the Lineweaver--Burk plot theorem, recalling Equation (25) and substituting we have:

$$\frac{1}{R} = \frac{k_s}{R_{max}[S]} + \frac{1}{R_{max}}, \frac{1}{R} = \frac{-39285.71}{-1190.48[S]} + \frac{1}{-1190.48}, \frac{1}{R} = \frac{32.99}{[S]} - 8.40E - 04$$

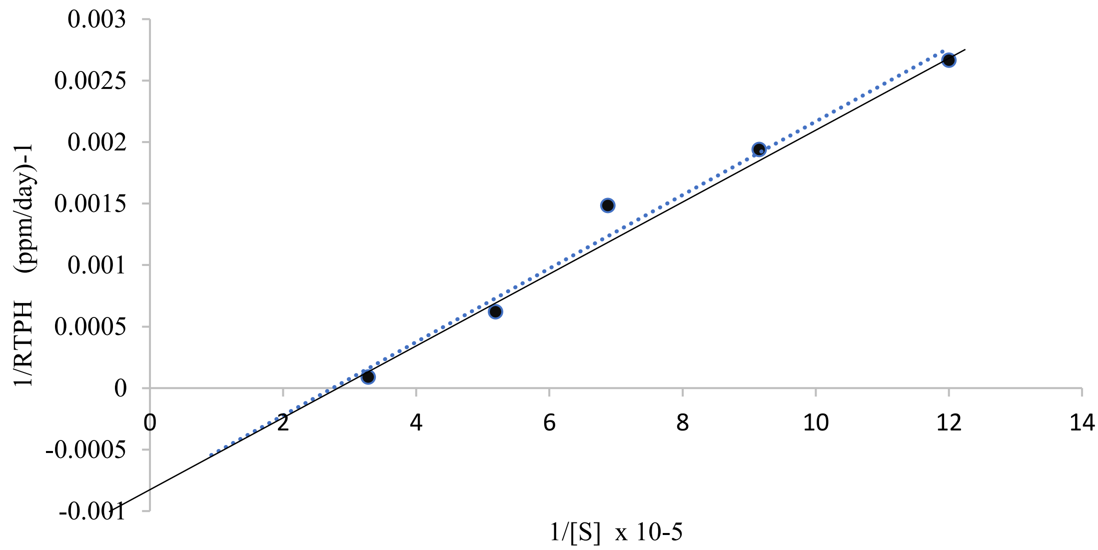

Figure 6. Lineweaver–Burk plot of $1/R_{TPH}$ vs. 1/[S] for bio-stimulant of room dried of 60 g dosage.

Similarly, Figure 6 expresses the graphical relationship of the reciprocal specific rate ($1/R_{TPH}$) of TPH decomposition with varying substrate concentration [S] over time using 60 g dosage of room-dried bio-stimulant of *Citrus sinensis* peel. From the intercept and slope of the graph, we can determine the maximum specific rate R_{max} of TPH degradation and equilibrium constant. The negative intercept read off the graph suggests a non-compliance to the Lineweaver–Burk plot theorem. Again, for the purpose of evaluating and determining the functional parameters and coefficient, the concept of Ukpaka was adopted.

Recalling from equation (25), the Lineweaver–Burk plot concept thus:

$$\frac{1}{R} = \frac{k_s}{R_{max}[S]} + \frac{1}{R_{max}}$$

where $\frac{1}{R_{max}}$ = intercept and $\frac{k_s}{R_{max}}$ = slope.

Here, $\frac{1}{R_{max}}$ = –0.0008 and R_{max} = 1/0.0008 = –1250

Since $\frac{k_s}{R_{max}} = slope$, therefore, $K_S = R_{max}$ (slope)

Computed slope from Figure 5: slope = (0.0028 -- 0.001)/(12.0 – 6.0) x 10^{-5} = 30.

K_S = –1250 * (30) = –37500 $(ppm)^{-1}$

Substituting values into the Lineweaver–Burk plot concept we have

$$\frac{1}{R} = \frac{-37500}{-1250 * [S]} + \frac{1}{-1250}$$

$$\frac{1}{R} = \frac{30}{[S]} - 8.0E - 04$$

And the Michaelis Menten equation for the 60 g dosage for the room-dried remediant is expressed as:

$$R_{A3} = \frac{[R_{A3}]_{max}[S]}{k_s + [S]}, R_{A3} = \frac{-1250 * [S]}{-37500 + [S]}$$

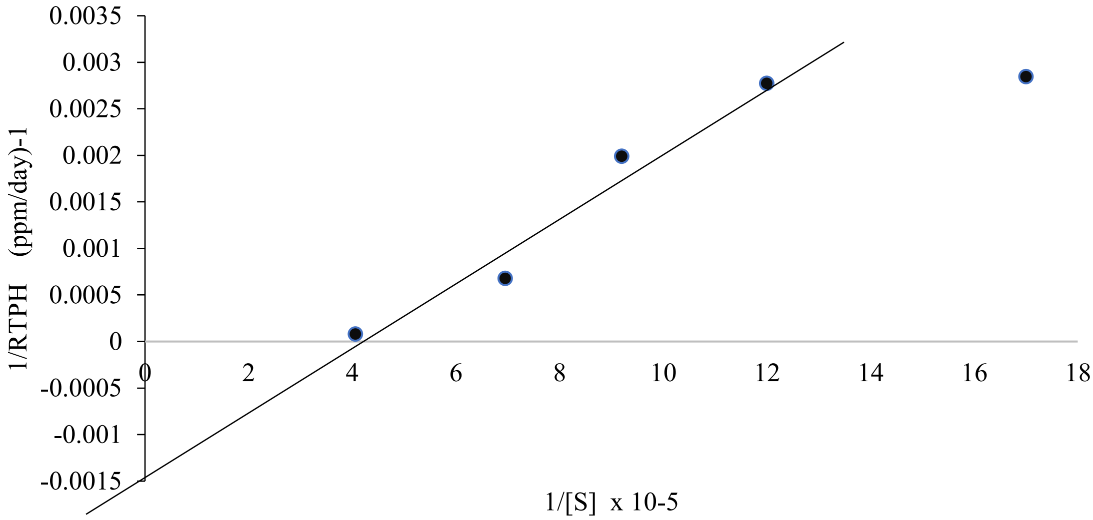

Figure 7. Lineweaver--Burk plot of $1/R_{TPH}$ vs. 1/[S] for bio-stimulant of room dried of 80 g dosage.

The plot of the reciprocal specific rate ($1/R_{TPH}$) of TPH decomposition with variation in substrate [S] reciprocal as shown in Figure 7 which identifies the Lineweaver–Burk plot for room-dried bio-stimulant of *Citrus sinensis* peel of 80 g dosage. Though a straight-line graph is obtained, however, the negative reading of the intercept implies maximum specific rate R_{max} of TPH degradation to be negative also and this is not compliant to the Lineweaver–Burk plot theorem. The functional parameters and coefficients were determined based on the Ukpaka's concept.

Recalling, the Lineweaver--Burk plot concept thus:

$$\frac{1}{R} = \frac{k_s}{R_{max}[S]} + \frac{1}{R_{max}}$$

where $\frac{1}{R_{max}}$ = intercept and $\frac{k_s}{R_{max}}$ = slope

From the graph of Figure 6, $\frac{1}{R_{max}}$ = –0.0015 and R_{max} = 1/0.0015= –666.6667

Also, since $\frac{k_s}{R_{max}} = slope$ and $K_s = R_{max}$ * (slope)

Determining the slope from the graph of Figure 6, we have

Slope = – (0.00278 – 0.00065)/(12.0 – 6.0) x 10^{-5} = 35.5

Thus, K_s = –666.6667 * (35.5) = –23666.6667 $(ppm)^{-1}$

Substituting values into the Lineweaver–Burk plot equation we have

$$\frac{1}{R} = \frac{-236666.6667}{-666.6667 * [S]} + \frac{1}{-666.6667}$$

$$\frac{1}{R} = \frac{35.5}{[S]} - 1.5E - 03$$

And the Michaelis Menten equation for the 80 g dosage for the room dried remediant is expressed as:

$$R_{A4} = \frac{[R_{A4}]_{max}[S]}{k_s + [S]}$$

The equation obtained is

$$R_{A4} = \frac{-666.67 * [S]}{-23666.67 + [S]}$$

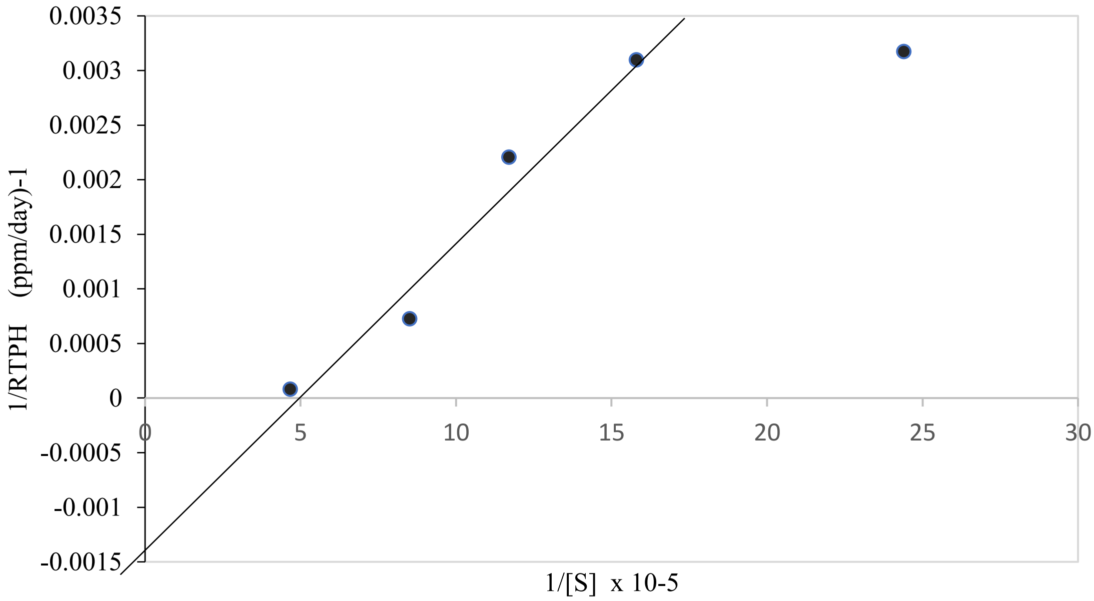

Figure 8. Lineweaver--Burk plot of $1/R_{TPH}$ vs. 1/[S] for bio-stimulant of room dried of 100 g dosage.

In determining the compliance of the 100 g dosage of room-dried bio-stimulant of *Citrus sinensis* peel, the reciprocal of the specific rate ($1/R_{TPH}$) of TPH reduction was plotted against the reciprocal of variation in substrate 1/[S] as seen in Figure 8. The straight-line graph showed a negative intercept implying the specific maximum rate of TPH reduction to be negative and further suggesting it does not follow the Lineweaver--Burk plot theorem. However, for purposes of this research, the Ukpaka's concept was adopted in determining the functional parameters and coefficients.

Recalling equation of the Lineweaver–Burk plot concept thus:

$$\frac{1}{R} = \frac{k_s}{R_{max}[S]} + \frac{1}{R_{max}}$$

where $\frac{1}{R_{max}}$ = intercept and $\frac{k_s}{R_{max}}$ = slope

From the graph represented in Figure 7, the intercept is read off as: $\frac{1}{R_{max}}$ = –0.0014.

Thus, R_{max} = 1/(--0.0014) = –714.285714 $(ppm/day)^{-1}$

Since $\frac{k_s}{R_{max}} = slope$ then, $K_s = R_{max}$ * (slope)

Also, the slope computed from the graph of Figure 7 is thus:

Slope = –(0.0031 – 0.0015)/(15.8 – 10.0) x 10^{-5} = 27.6

And, K_s=–714.2857 * (27.6) = –19714.2857 $(ppm)^{-1}$

Substituting these values into the Lineweaver–Burk plot equation we have

$$\frac{1}{R} = \frac{-19714.2857}{-714.2857 * [S]} + \frac{1}{-7142857}$$

$$\frac{1}{R} = \frac{27.6}{[S]} - 1.4E - 03$$

And the Michaelis Menten equation for the 100 g dosage for the room-dried remediant is expressed as:

$$R_{A5} = \frac{[R_{A5}]_{max}[S]}{k_s + [S]}$$

$$R_{A5} = \frac{-714.29 * [S]}{-19714.29 + [S]}$$

Figure 9 is an illustration of the relationship between the reciprocals of the specific rate R_{TPH} of TPH degradation naturally occurring with variation in substrate [S] over time. A straight-line graph with positive intercept is a strong indication of a compliance with the Lineweaver–Burk plot theorem. The positive intercept implies a positive rate of decomposition.

Recalling, the Lineweaver–Burk plot concept from Equation (25) thus:

$$\frac{1}{R} = \frac{k_s}{R_{max}[S]} + \frac{1}{R_{max}}$$

where $\frac{1}{R_{max}}$ = intercept and $\frac{k_s}{R_{max}}$ = slope

Here, $\frac{1}{R_{max}}$ = 0.0014; thus, R_{max} = 1/0.0014 = 714.285714

Since $\frac{k_s}{R_{max}} = slope$ then, $K_S = R_{max}$* (slope)

Slope = (0.00335 – 0.0031)/(2.4 – 2.1) x 10^{-5} = 83.3

K_S = 714.285714 * (83.3) = 59500 $(ppm)^{-1}$

Substituting these values into the Lineweaver–Burk plot equation we have

$$\frac{1}{R} = \frac{59500}{714.2857 * [S]} + \frac{1}{714.2857}$$

$$\frac{1}{R} = \frac{83.3}{[S]} + 1.4E + 03$$

And the Michaelis Menten equation for the control without the input of any remediant is given as:

$$R_{C1} = \frac{[R_{C1}]_{max}[S]}{k_s + [S]}$$

$$R_{C1} = \frac{714.29 * [S]}{59500 + [S]}$$

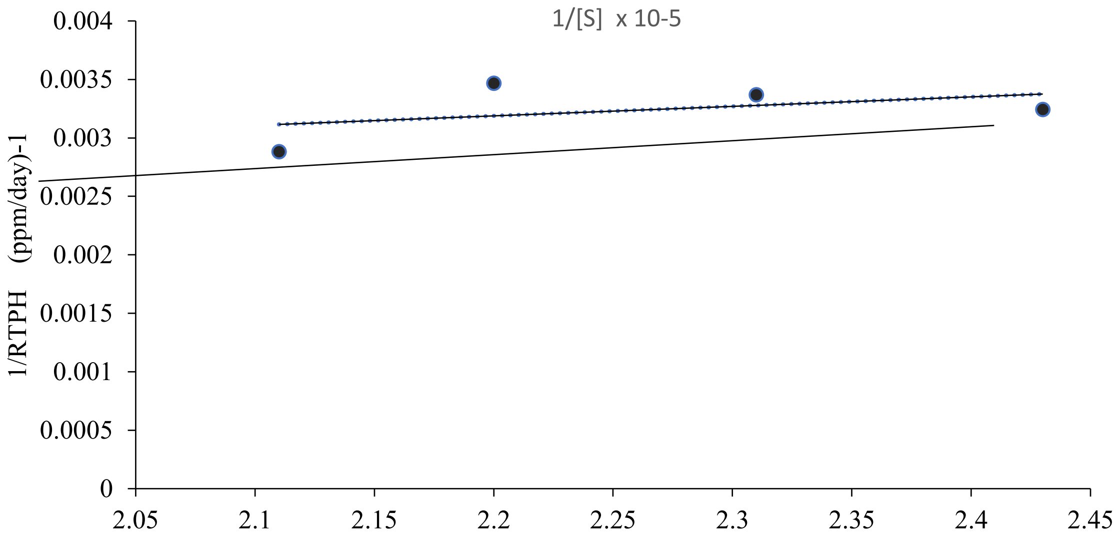

Figure 9. Lineweaver--Burk plot of $1/R_{TPH}$ vs. 1/[S] for control of 0 g dosage remediant.

Relationship of InS_{TPH} and Time for Bio-stimulant of Room-Dried Application and Control Sample

Figure 10 shows the relationship of InS_{TPH} and time of room dried sample of remediant (20 g dosage). Decrease in the InS_{TPH} was seen with increase in time. Recall the equation for a first order reaction is as expressed in equations below:

$S_{TPH(t)} = S_{TPH(0)}e^{-k_1 t}$ and $InS_{TPH(t)} = InS_{TPH(0)} - K_1 t$

where, $InS_{TPH(0)}$ = intercept and $-K_1$ = Slope.

Reading from the regression equation of y = –0.0382x + 10.931, thus: $-K_1 = -0.0382$ and In $S_{TPH(0)}$ = 10.931.

Substituting values into the Equation (21), we have

$InS_{TPH(t)} = InS_{TPH(0)} - K_1 t$, we have a relationship for the degradation TPH using 20 g dosage of room-dried *Citrus sinensis* expressed as:

$InS_{TPH(A1,t)} = 10.931 – 0.0382 * t$

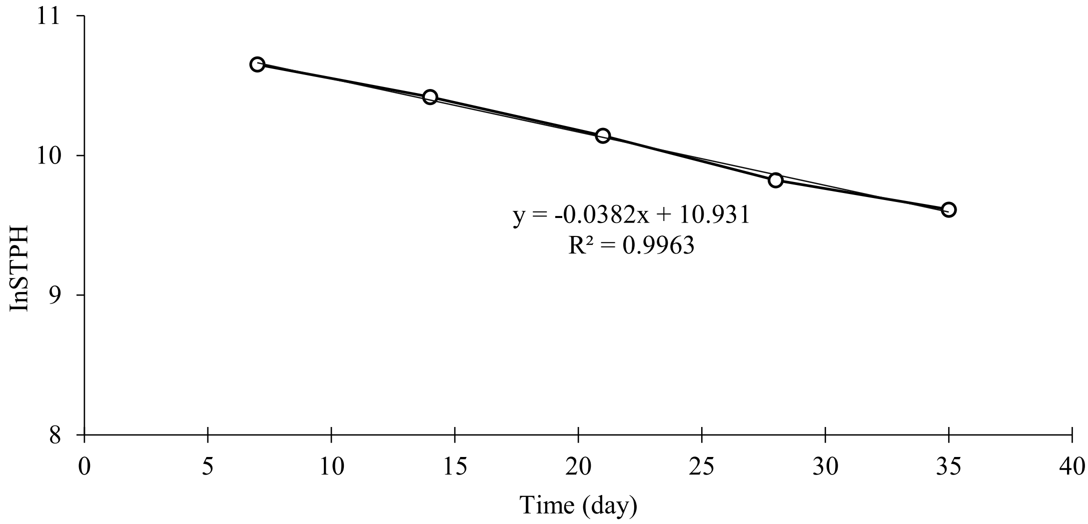

Figure 10. Plot of InS_{TPH} versus time for room dried of *Citrus sinensis* peel of 20 g dosage.

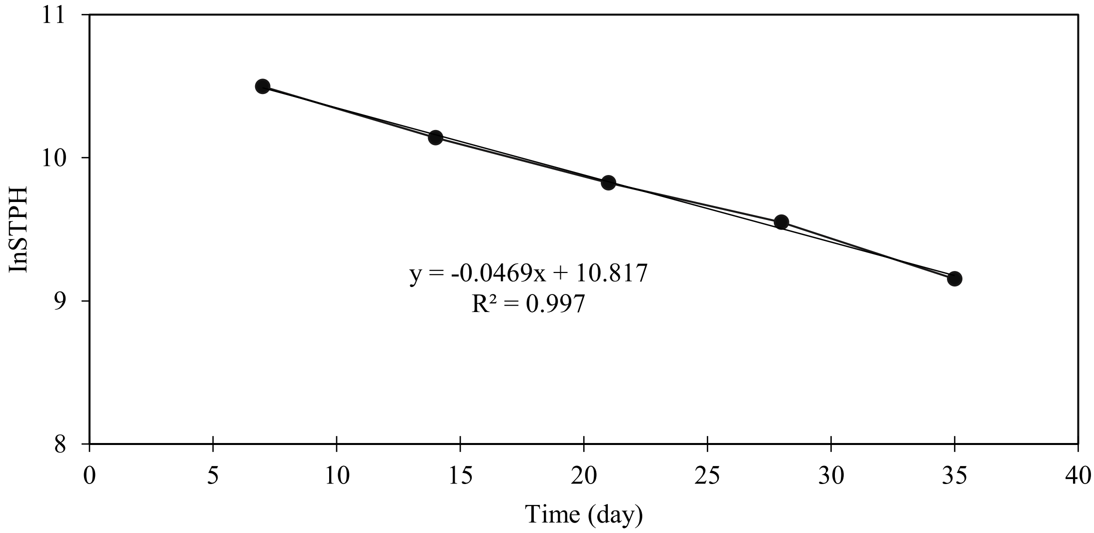

Figure 11. Plot of InS_{TPH} versus time for room dried of *Citrus sinensis* peel of 40 g dosage.

The relationship of InS_{TPH} and Time of A2-room dried sample of remediant (40 g dosage) is represented graphically in Figure 10(a). Decreasing values of InS_{TPH} was observed with increasing time. Recall the equation for first order reaction is as expressed in Equations (20 & 21),

$$S_{TPH(t)} = S_{TPH(0)} e^{-k_1 t}$$

$S_{TPH(0)} e^{-k_1 t}$ and $InS_{TPH(t)} = InS_{TPH(0)} - K_1 t$

where $InS_{TPH(0)}$ = intercept and $-K_1$ = Slope

Therefore, from the regression equation obtained of y = –0.0469x + 10.817,

$-K_1 = -0.0469$; and In $S_{TPH(0)} = 10.817$

Substituting these values into Equation (21) we have a mathematical equation developed for the 40 g dosage *Citrus sinensis* peel and its expressed as:

$InS_{TPH(A2,t)} = 10.817 - 0.0469 * t$

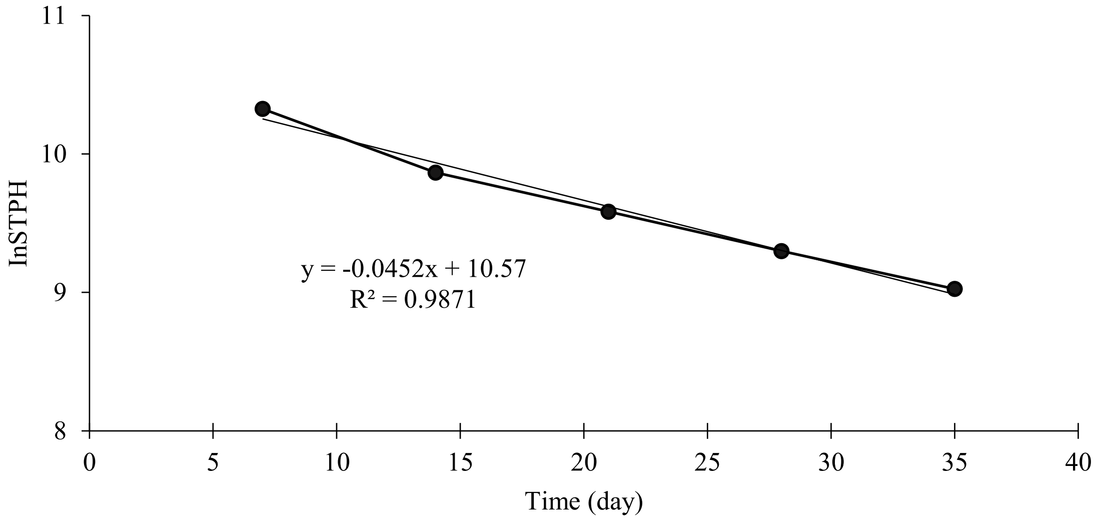

Figure 11. Plot of InS_{TPH} versus time for room dried of citrus sinensis peel of 60 g dosage.

The illustration of InS_{TPH} versus time is seen in Figure 11 for the 60 g dosage of the room-dried sample of remediant of *Citrus sinensis*. The InS_{TPH} is seen to decrease in value with increase in time. Recall the equation for a first order reaction is as expressed in equations below:
$S_{TPH(t)} = S_{TPH(0)}e^{-k_1 t}$ and $InS_{TPH(t)} = InS_{TPH(0)} - K_1 t$

Where $InS_{TPH(0)}$ = intercept and $-K_1$ = Slope

The straight line relationship observed from the graph gives a regression equation of y = –0.0452x + 10.57, corresponding to: $-K_1 = -0.0452$ and In $S_{TPH(0)} = 10.57$.

Substituting these values into Equation (21) we obtain the degradation equation for the 60 g dosage of room-dried remediant expressed as:
$InS_{TPH(A3,t)} = 10.57 - 0.0452 * t$

Figure 12 demonstrates the relationship of InS_{TPH} and time of room-dried sample of remediant (80 g dosage). Decrease in the values of InS_{TPH} is observed with increase in time. Recall the equation for a first order reaction is as expressed in equations below:
$S_{TPH(t)} = S_{TPH(0)}e^{-k_1 t}$ or $InS_{TPH(t)} = InS_{TPH(0)} - K_1 t$

where $InS_{TPH(0)}$ = intercept and $-K_1$ = Slope.

Therefore, from the regression equation of y = –0.0487x + 10.36,

thus, –K1 = –0.0487, and In $S_{TPH(0)} = 10.36$

Substituting these values into the equation, we have the mathematical expression for the room-dried remediant of 80 g dosage:

$InS_{TPH(A4,t)} = 10.36 - 0.0487 * t$

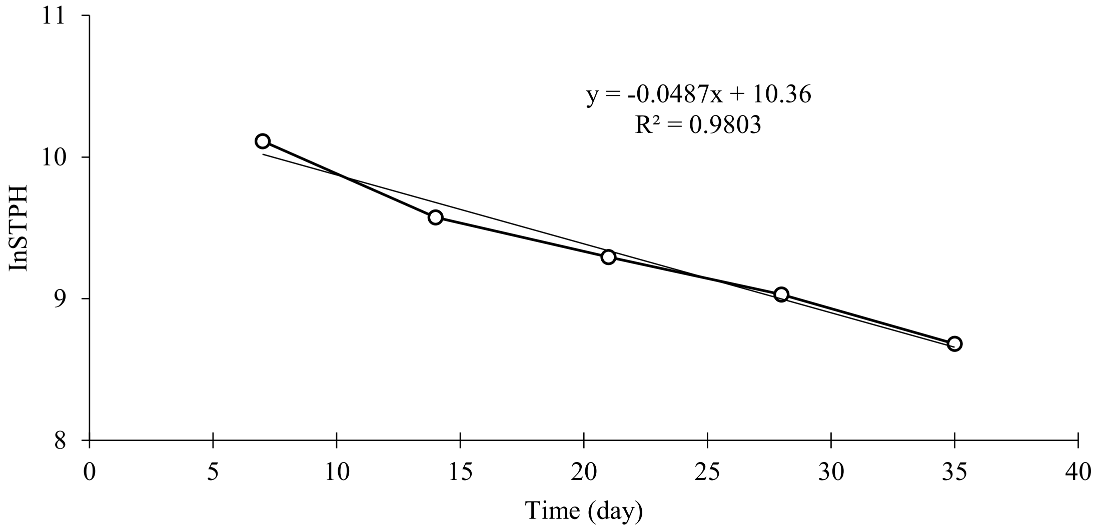

Figure 12. Plot of InS_{TPH} versus time for room-dried of *Citrus sinensis* peel of 80 g dosage.

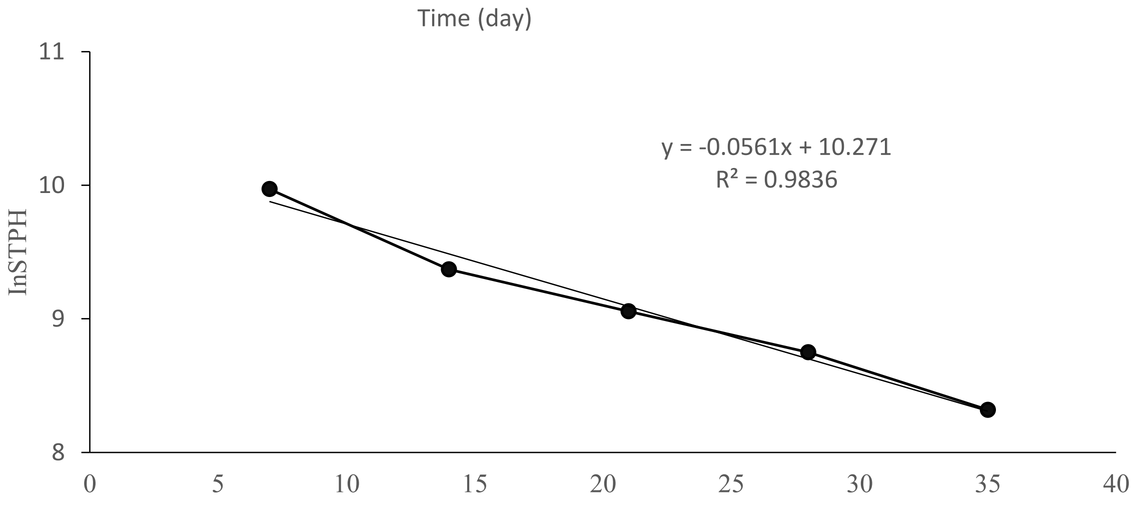

Figure 13. Plot of InS_{TPH} versus time for room-dried of *Citrus sinensis* peel of 100 g dosage.

Figure 13 shows the relationship of the natural log of the substrate InS_{TPH} using room-dried sample of 100 g dosage remediant over a period a decreasing trend is observed in the InS_{TPH} as time increases. Recall the equation for a first order reaction is as expressed in equations below:

$S_{TPH(t)} = S_{TPH(0)}e^{-k_1 t}$ and $InS_{TPH(t)} = nS_{TPH(0)} - K_1 t$

where $InS_{TPH(0)}$ = intercept and $-K_1$ = Slope

Therefore, from the regression equation of y = -0.0561x + 10.271, thus, $-K_1 = -0.0561$ and $In\ S_{TPH(0)} = 10.271$

Substituting these values into the Equation (21), we have the mathematical equation for the room-dried 100 g remediant as:

$InS_{TPH(A5,t)} = 10.271 – 0.0561 * t$

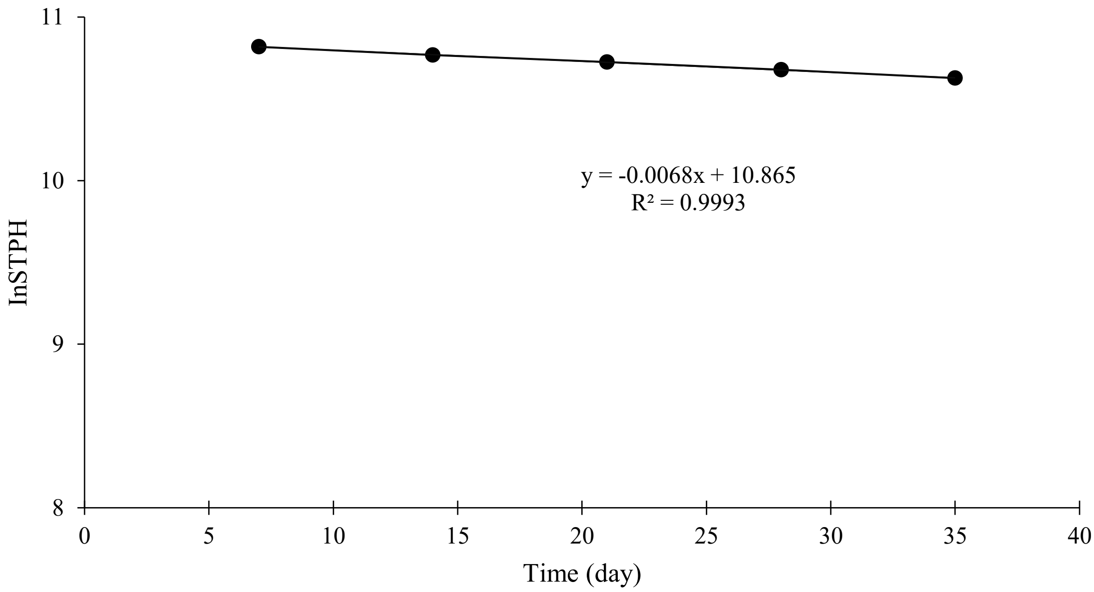

Figure 14. Plot of InS_{TPH} versus time for control with 0 g dosage of *Citrus sinensis* peel.

Figure 14 represents a graphical relationship of natural log of the controlled substrate InS_{TPH} over the Time duration of the experiment with no remediant added. A decrease in the InS_{TPH} values is observed over the time duration of the entire experiment. We would recall the equation for a first order reaction is as expressed in Equations (20 and 21).

$S_{TPH(t)} = S_{TPH(0)}e^{-k_1t}$ and $InS_{TPH(t)} = InS_{TPH(0)} - K_1t$

where $InS_{TPH(0)}$ = intercept and $-K_1$ = Slope.

Reading values from the regression equation of y = –0.0068x + 10.865,

we have, –K1 = –0.0068 and In $S_{TPH(0)}$ = 10.865.

Substituting these values into Equation (21), we have:

$InS_{TPH(C1, t)} = 10.865 – 0.0068 * t$

Relationship of InS_{TPH} and Time for Bio-stimulant of Sun-Dried Application and Control Sample

Figure 15 expresses the graphical relationship of the natural log of the substrate InS_{TPH} using sun-dried sample of 20 g dosage remediant over a period. As observed with the room-dried remediant, a similar decreasing trend is observed in the InS_{TPH} over the time of the experiment. Recall the equation for a first order reaction is as expressed in Equations (20 & 21)

$S_{TPH(t)} = S_{TPH(0)}e^{-k_1t}$ and $InS_{TPH(t)} = InS_{TPH(0)} - K_1t$

where $InS_{TPH(0)}$ = intercept and $-K_1$ = Slope

From the regression equation of y = –0.0366x + 10.996, as expressed in Figure 14 we have:

$-K1 = -0.0366$ and $\text{In } S_{TPH(0)} = 10.996$

Substituting these values into the Equation (21) we have a mathematical expression for sun-dried remediant of 20 g dosage:

$\text{In}S_{TPH(B1,t)} = 10.996 -- 0.0366 * t$

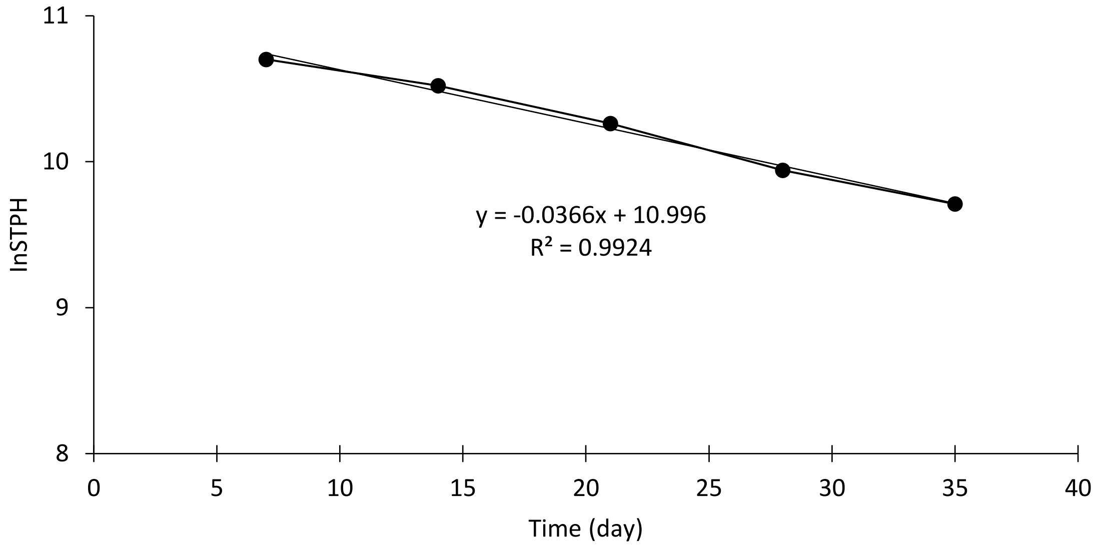

Figure 15. Plot of $\text{In}S_{TPH}$ versus time for sun-dried of *Citrus sinensis* peel of 20 g dosage.

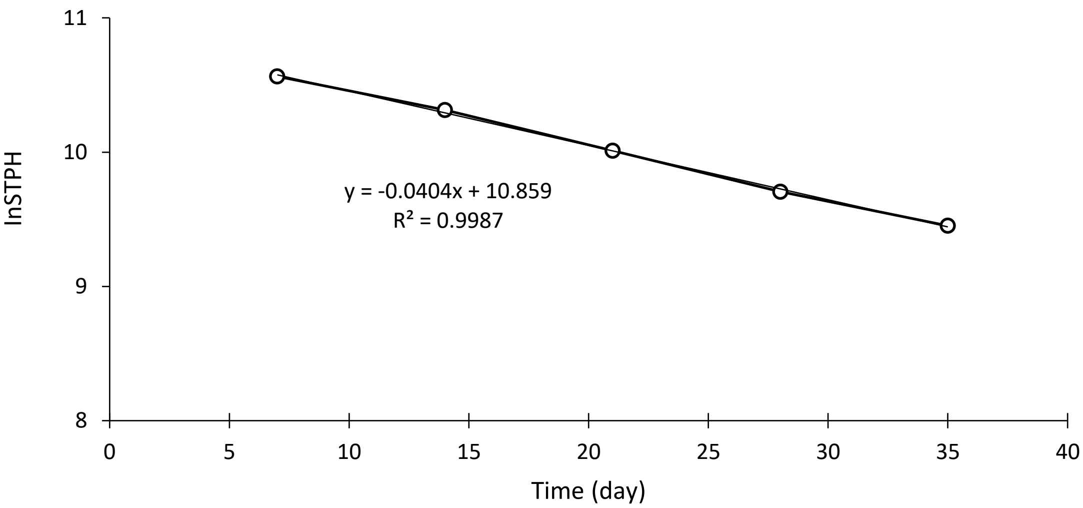

Figure 16. Plot of $\text{In}S_{TPH}$ versus time for room-dried of *Citrus sinensis* peel of 40 g dosage.

Illustrating the relationship of $\text{In}S_{TPH}$ and time of sun-dried sample of 40 g remediant dosage. Decrease in the values of $\text{In}S_{TPH}$ is observed with increase in time. Recall the equation for a first order reaction is as expressed in Equations (20 & 21) and in Figure 16.

$S_{TPH(t)} = S_{TPH(0)}e^{-k_1 t}$ and $InS_{TPH(t)} = InS_{TPH(0)} - K_1 t$

where $InS_{TPH(0)}$ = intercept and $-K_1$ = Slope.

Reading from the graph of Figure 15, the regression equation, y = –0.0404x + 10.859,
Thus, –K1 = –0.0404 and In $S_{TPH(0)}$ = 10.859.

Substituting these values into the Equation (21), we have a mathematical expression for sun-dried remediant of 40 g dosage:

$InS_{TPH(B2,t)}$ = 10.859 – 0.0404 * t.

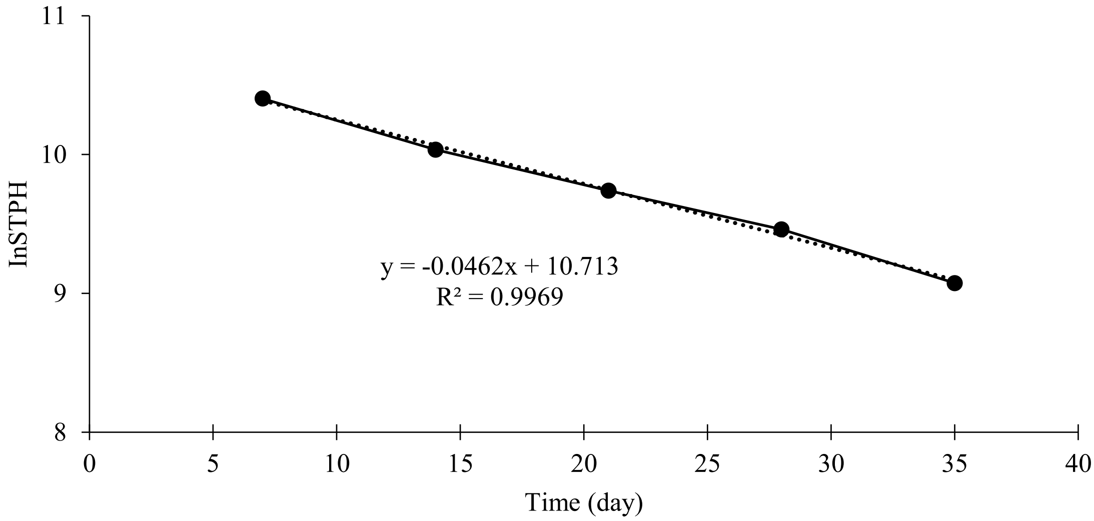

Figure 17. Plot of InS_{TPH} versus time for sun-dried of *Citrus sinensis* peel of 60 g dosage.

The relationship of InS_{TPH} and time of 60 g dosage of sun-dried sample of remediant is represented graphically in Figure 17. The decreasing values of InS_{TPH} was observed over increasing time range.

Recall the equation for first order reaction is as expressed in Equations (20 & 21)

$S_{TPH(t)} = S_{TPH(0)}e^{-k_1 t}$ or $InS_{TPH(t)} = InS_{TPH(0)} - K_1 t$

where $InS_{TPH(0)}$ = intercept and $-K_1$ = Slope

Therefore, from the regression equation of y = –0.0462x + 10.713

Thus, –K1 = –0.0462 and In $S_{TPH(0)}$ = 10.713

Substituting these values into the equation, we have the mathematical expression for the sun-dried remediant of 60 g dosage,

$InS_{TPH(B3,t)}$ = 10.713 – 0.0462 * t

Figure 18 shows the relationship of the natural log of the substrate InS_{TPH} using sun-dried sample of 80 g dosage remediant over a period. A decreasing trend is observed in the InS_{TPH} as time increases. Recall the equation for a first order reaction is as expressed in Equations (20 & 21).

$S_{TPH(t)} = S_{TPH(0)}e^{-k_1 t}$ and $InS_{TPH(t)} = nS_{TPH(0)} - K_1 t$

where $InS_{TPH(0)}$ = intercept and $-K_1$ = Slope

Therefore, from the regression equation of y = –0.0458x + 10.465, thus, –K1 = –0.0458 and $InS_{TPH(0)}$ = 10.465

Substituting these values into the equation, we have the mathematical expression for the sun-dried remediant of 80 g dosage,

$InS_{TPH(B4,t)}$ = 10.465 – 0.0458 * t

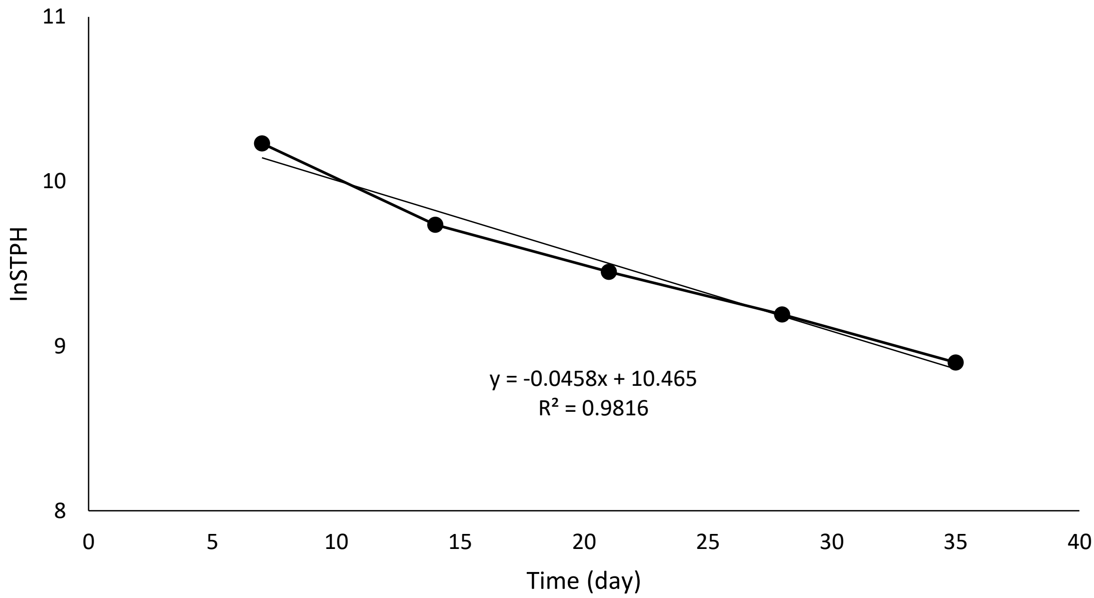

Figure 18. Plot of InS_{TPH} versus time for sun-dried of *Citrus sinensis* peel of 80 g dosage.

Figure 19 represents a graphical relationship of natural log of the substrate with 100 g dosage of sun-dried remediant InS_{TPH} over the time duration of the experiment. A decrease in the InS_{TPH} values is observed over the time duration of the entire experiment. The equation would be recalled for a first order reaction is as expressed in Equations (20 & 21):

$S_{TPH(t)} = S_{TPH(0)}e^{-k_1 t}$ and $InS_{TPH(t)} = InS_{TPH(0)} - K_1 t$

where $InS_{TPH(0)}$ = intercept and $-K_1$ = Slope

Reading values from the regression equation of y = –0.0531x + 10.269,

we have, $–K_1$ = –0.0531 and In $S_{TPH(0)}$ = 10.269.

Substituting these values into the equation, we have the mathematical expression for the sun-dried remediant of 100 g dosage:

$InS_{TPH(B5,t)}$ = 10.269 – 0.0531 * t.

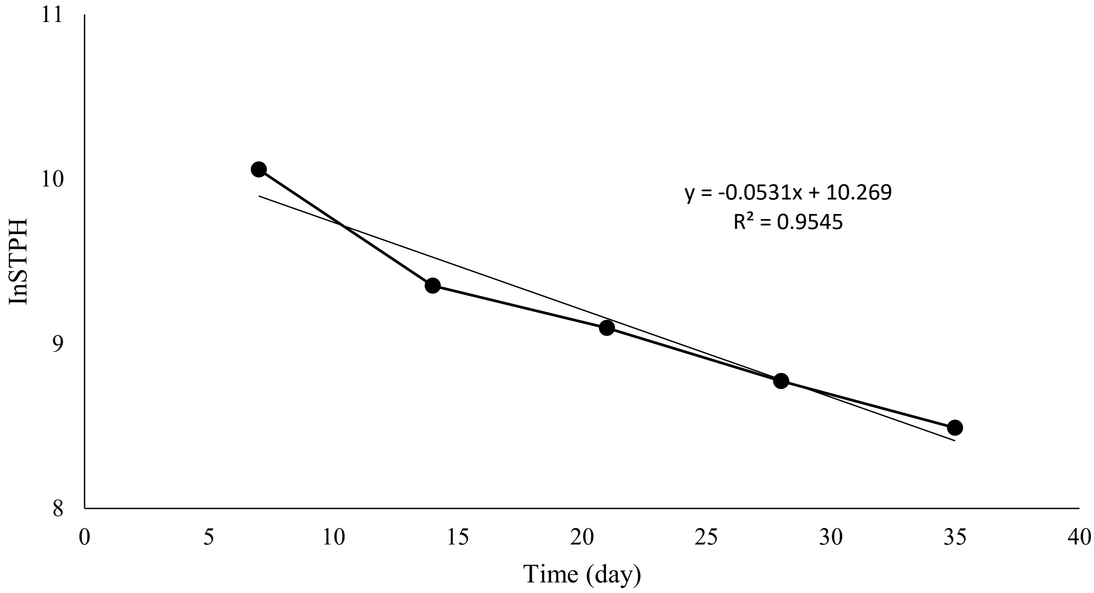

Figure 19. Plot of InS_{TPH} versus time for sun-dried of *Citrus sinensis* peel of 100 g dosage.

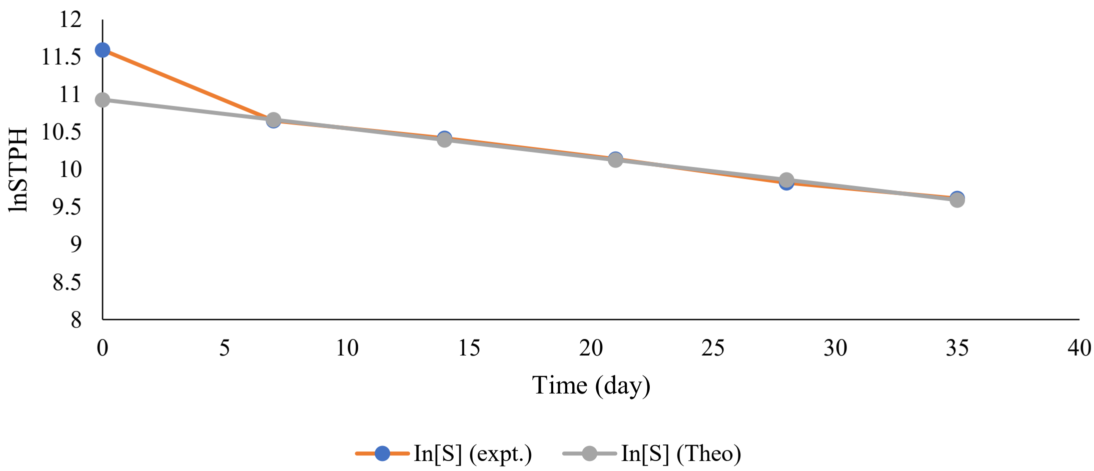

Figure 20. Comparison of experimental and theoretical value of InS_{TPH} versus time for 20 g dosage of remediation of room-dried sample.

Comparison of Experimental and Theoretical of InS_{TPH} and Time for Bio-stimulant of Room-Dried Application and Control Sample

Figure 20 shows the behavior of the theoretical and experimental value of InS_{TPH} with variation in time. Decrease in InS_{TPH} was experienced with increase in time. However, a comparison of the theoretical value with experimental value reveals that the trend of InS_{TPH} is in the same manner and shows a good match; implying that the regression model of the plot can be used to predict the characteristics of crude oil degradation using the *Citrus sinensis* (orange) peel as a remediant.

A comparison of the theoretical plot against the experimental plots of InS_{TPH} over the time duration of the experiment as depicted in Figure 21 for the 40 g remediant demonstrates not only a similar trend of decreasing values of InS_{TPH} with increasing time, but also closely related values of InS_{TPH} with corresponding time as seen in the table of values. This reveals that the regression model obtained from the plot can be used to predict the degradation characteristics of the crude oil using the peel of orange (*Citrus sinensis*).

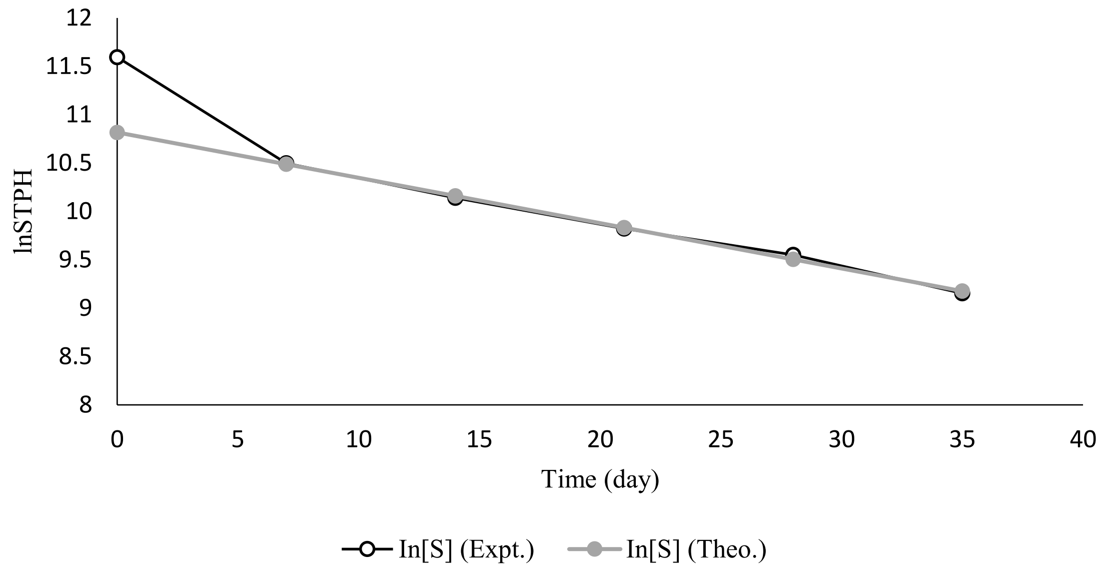

Figure 21. Comparison of experimental and theoretical value of InS_{TPH} versus time for 40 g dosage of remediation of room-dried sample.

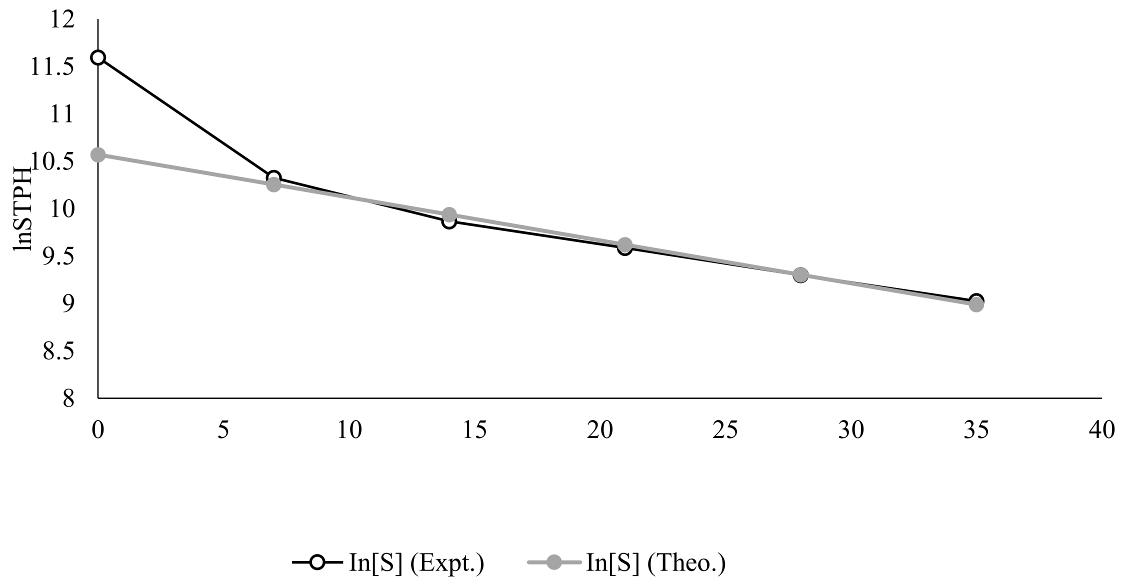

Figure 22. Comparison of experimental and theoretical value of InS_{TPH} versus time for 60 g dosage of remediation of room-dried sample.

Demonstrating the relationship between InS_{TPH} and time for both the experimental data and the computed data for 60 g dosage of remediant (*Citrus sinensis* peel) is Figure 22. Both data sets exhibit similarities in the decreasing values of InS_{TPH} with increasing Time. The computed values show a very good correlation with the experimental data set further affirming that the regression model developed can be used to predict the characteristics of crude oil degradation using the *Citrus sinensis* (orange) peel as a remediant.

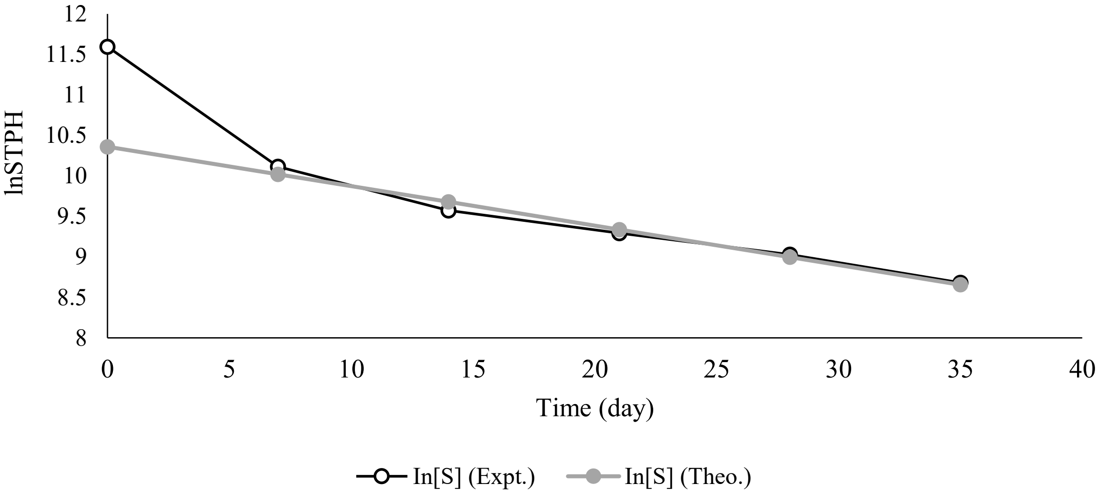

Figure 23. Comparison of experimental and theoretical value of InS_{TPH} versus time for 80 g dosage of remediation of room-dried sample.

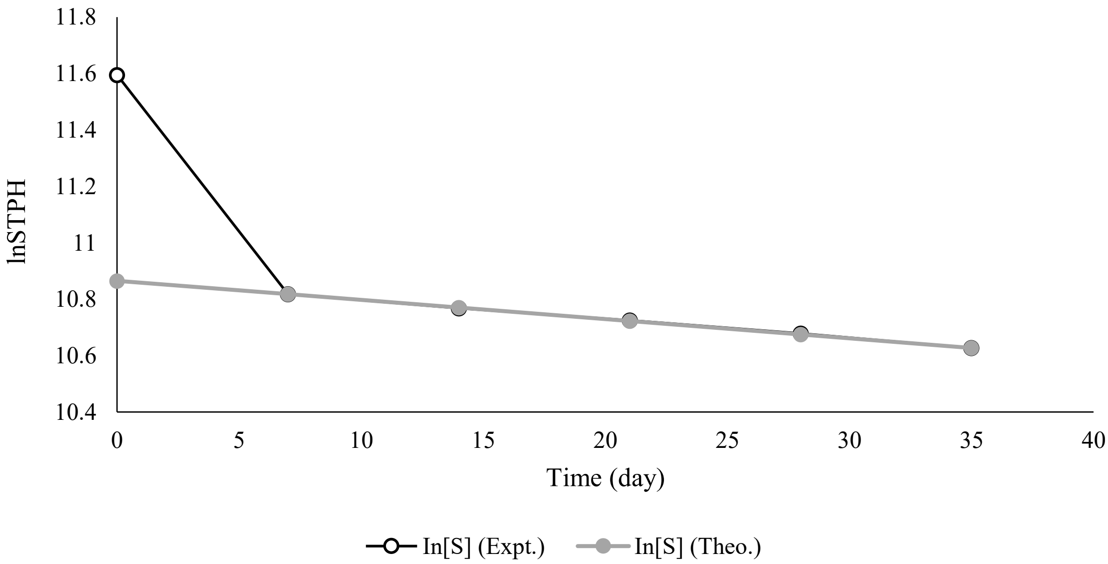

Figure 24. Comparison of experimental and theoretical value of InS_{TPH} versus time for 100 g dosage of remediation of room-dried sample.

Figure 23 illustrates the graphical representation of InS_{TPH} with time for both the experimental values and the theoretical values, both have similar behavioral pattern of decreasing values of InS_{TPH} with increasing time and closely matched figures demonstrating a good correlation. Thus, suggesting that the mathematical model developed can be used to predict the mitigation characteristics of the crude oil when orange peel is used as remediant.

Similarly, Figure 24 depicts a plot of InS_{TPH} with time for both the experimental values and the theoretical values, both have similar behavioral pattern of decreasing values of InS_{TPH} with increasing time and closely matched figures demonstrating a good correlation. Further, collaborating that the mathematical model developed can be used to predict the decomposition characteristics of the crude oil when orange peel is used as remediant.

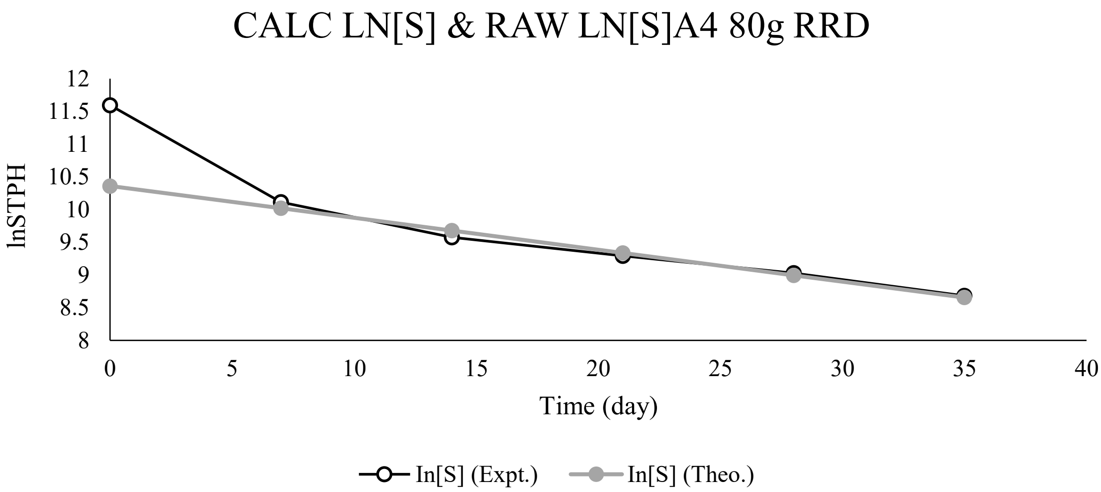

Figure 25. Comparison of experimental and theoretical value of InS_{TPH} versus time for control.

Figure 25 illustrates the graphical representation of InS_{TPH} with time for both the experimental values and the theoretical values, both have similar behavioral pattern of decreasing values of InS_{TPH} with increasing time and closely matched figures demonstrating a good correlation. Thus, suggesting that the mathematical model developed can be used to predict the mitigation characteristics of the crude oil when orange peel is used as remediant.

CONCLUSION

Research was conducted to determine the biokinetic parameters of crude oil degradation using *Citrus sinensis* (orange) peel as a bio-stimulant. The loamy soil sample was contaminated with crude oil and the bio-stimulant added for the purpose of remediation. The process was examined in line with the aim and objectives of the research as illustrated in the conclusion as shown below.

The experimental set-up was monitored by examining the TPH concentration with time intervals and the research demonstrates decrease in the TPH concentration with increase in time. This revealed a progressive cost-efficient and process-efficient bioremediation option for hydrocarbon-contaminated soils.

The rate of TPH degradation in each bioreactor set-up was determined using the established mathematical model is presented in this research. The decay rate constant parameter for each bioreactor was determined as shown in this research and the variation in the decay rate K_1 or K_d was attributed to the effectiveness of the bio-stimulant. The variation in the value of the decay rate was experienced with bio-stimulant of sun dry and room dry. However, the research revealed that higher mitigation was observed with the room dry than the sun dry. The reason being that the room dry bio-stimulant contains high percentage of nutrient values.

Finally, the biokinetic parameters and coefficients were determined by recalling the Michaelis Menten model, rate equation model of first and second order as well as the Monod's model equation. The specific rate of the TPH degradation, maximum specific rate of TPH and equilibrium constant of TPH as well as the rate decay of TPH was evaluated and determined as shown in this research.

REFERENCES

1. Abdul-Kareem R, Gnansounou C, Adongo RS. Effects of the oil-find on land management in the Sekondi-Taroradi Metropolis, Western Coast of Ghana. J Land Use Sci. 2021;16(4):398–412.
2. Adeniyi AG, Abdulkareem S, Iwuozor KO, Ogunniyi S, Abdulkareem MT, Emenike EC, Sagboye PA. Effect of salt impregnation on the properties of Orange Albedo Biochar. Chem Life Cycle. 2022. doi:10.1016/j.clce.2022.100059.
3. AFP. Oil cleanup in southern Nigeria still a "long way" from target. Phys Org. 2021. https://phys.org/news/2021-10-oil-cleanup-southern-nigeria.html.
4. Ahmad AA, Muhammad I, Shah T, Kalwar Q, Zhang J, Liang Z, Mei D, Juanshan Z, Yan P, Zhi DX, Rui-Jun L. Remediation methods of crude oil contaminated soil. World J Agric Soil Sci. 2020. doi:10.33552/WJASS.2020.04.000595.
5. Ajua F, Ukpaka CP. Study on crude oil remediation on soil environment using fermented Cassava Liquid. J Chem Eng Process Technol. 2020;6(2):1045--1054.
6. Albert ON, Amaratunga D, Haigh RP. Evaluation of impacts of oil spill disaster on communities and its influence on Restiveness in Niger Delta, Nigeria. Proc Eng. 2018;212:1054–61. doi:10.1016/j.proeng.2018.01.136.
7. Ambaye TG, Chebbi A, Formicola F, Prasad S, Gomez FH, Franzetti A, Vaccari M. Remediation of soil polluted with Petroleum Hydrocarbons and its reuse for agriculture: Recent progress, challenges, and perspectives. Chemosphere. 2022;293:13377. doi:10.1016/j.chemosphere.2022.133572.
8. Bebeteidoh OL, Kometa S, Pazouki K, Norman R. Sustained impact of the activities of local crude oil refiners on their host communities in Nigeria. Heliyon. 2020;6(6). doi:10.1016/j.heliyon.2020.e04000.
9. Chen S, Zhong M. Bioremediation of petroleum-contaminated soil. In: Environmental chemistry and recent pollution control approaches. 2019. doi:10.5772/intechopen.90289.
10. Etebu E, Nwauzoma AB. A review on sweet orange (Citrus sinensis L. Osbeck): Health, diseases, and management. Am J Res Commun. 2014;2(2):33–70.
11. Gundlach ER. Oil-related mangrove loss East of Bonny River. In: Threats to Mangrove Forest. 2018;267–321. doi:10.1007/978-3-319-73016-5_13.
12. Leggett RW. Biokinetic modeling. In: Advanced radiation protection dosimetry. 2019;215–306.
13. Mba C. Only 2% of Oil spillages cleaned up in 5 years due to NOSDRA's dependent relationship on oil companies in Nigeria. Dataphyte. 2021. https://www.dataphyte.com/latest-reports/extractive/only-2-of-oil-spillages-cleaned-up-in-5-years-due-to-nosdras-dependent-relationship-on-oil-companies-in-nigeria/.
14. Mihali C, Dippong T, Dumuța A, Mureșan AR. Characterization of active compounds from Citrus Peels By-Products using Chromatographic and Optic methods. Sci Bull North Univ Cent Baia Mare. 2017;31(2):41–47.
15. Mnif S, Chebbi A, Mhiri N, Sayadi S, Chamkha M. Biodegradation of Phenanthrene by a bacterial Consortium Enriched from Sercina Oilfield. Process Saf Environ Prot. 2017;107:44–53.
16. Nwachukwu I, Mbachu IC. The socio-cultural implications of Crude Oil Exploration in Nigeria. In: The political ecology of oil and gas in the Nigerian Aquatic Ecosystem. 2018;177–190. doi:10.1016/B978-0-12-809399-3.00013-6.
17. Obuge AM, Ukpaka CP, Amadi SA, Puyate YT. Experimental based study of Justicia Carnea and Moringa oleifera extract on crude oil remediation of Contaminated Loamy soil. Int J Environ Chem. 2021;7(2):13–28.
18. 18.Ogunlade CA, Jekayinfa SO, Olaniran JA, Adebayo AO. Energy life-cycle assessment and economic analysis of sweet orange production in Nigeria. Agric Eng Int CIGR J. 2020;22(2):123–132.
19. Olatunji OM, Horsfall IT, Ekiyor TH. Comparison of bioremediation capabilities of poultry droppings and Avocado Pear Seed Cake in Petroleum polluted soil. J Eng Technol Res. 2018;10(5). doi:10.5897/jetr2018.0652.
20. Promise N, Ukpaka CP, Puyate Y. Biokinetics of crude oil remediation using Dogoyaro (Azadirachta indica) Stem. Indian J Eng. 2020;17(47):250–60.

21. Ratcliffe R. "This Place Used to Be Green": The Brutal Impact of Oil in the Niger Delta. The Guardian. 2019. https://www.theguardian.com/global-development/2019/dec/06/this-place-used-to-be-green-the-brutal-impact-of-oil-in-the-niger-delta.
22. Ren X, Zeng G, Tang L, Wang J, Wan J, Wang J, Deng Y, Liu Y, Peng B. The potential impact on the biodegradation of organic pollutants from composting technology for soil remediation. Waste Manag. 2018;72:138–49. doi:10.1016/j.wasman.2017.11.032.
23. Ruley JA, Amoding A, Tumuhairwe JB, Basamba TA. Rhizoremediation of Petroleum Hydrocarbon–Contaminated soils: A systematic review of mutualism between Phytoremediation species and soil living microorganisms. In: Phytoremediation. 2022;263–96. doi:10.1016/B978-0-323-89874-4.00008-X.
24. Shravan R, Shere DM, Joshi MM. Study of physico-chemical characteristics of sweet orange (Citrus sinensis) fruit. J Pharmacogn Phytochem. 2018;1687–89.
25. Ukhurebor KE, Athar H, Adetunji CO, Aigbe UO, Onyancha RB, Abifarin O. Environmental implications of Petroleum Spillages in the Niger Delta Region of Nigeria: A review. J Environ Manag. 2021;293. doi:10.1016/j.jenvman.2021.112872.
26. Ukpaka CP. Investigation into the Kinetics of Biodegradation of Crude Oil in different soils. J Eng Technol Res. 2012;4(2):33–48. doi:10.5897/jetr11.057.
27. Ukpaka CP, Udeh I. Kinetic Model for Crude Oil Degradation Using Moringa Extract. Int J Pet Eng. 2015;1(2):28–39. https://www.researchgate.net/publication/346930058_Kinetic_Model_for_Crude_Oil_Degradation_Using_Moringa_Extract.
28. Ukpaka C. Development of model for bioremediation of crude oil using moringa extract. Chem Int. 2016;2:19–28.
29. Ukpaka C. Comparison on the performance of Moringa and Neem Root Extracts on Crude Oil degradation in soils environment. Pet Petrochem Eng J. 2020;4(3):19.
30. Ukpaka CP, Ajua FN, Amadi SA. Biokinetics of Crude Oil Remediation on soil environment using fermented Cassava liquid. Int J Chem Mol Eng. 2020;6(2). https://chemical.journalspub.info/index.php?journal= JCME&page= article & op=view&path%5B%5D=1045

